Clays and Clay Minerals, Vol. 23, pp. 125–129. Pergamon Press 1975. Printed in Great Britain

MICACEOUS OCCLUSIONS IN KAOLINITE OBSERVED BY ULTRAMICROTOMY AND HIGH RESOLUTION ELECTRON MICROSCOPY

S. Y. LEE and M. L. JACKSON*

Department of Soil Science, University of Wisconsin, Madison, Wisconsin 53706, U.S.A.

and

J. L. BROWN†

Analytical Instrumentation Laboratories, Engineering Experiment Station, Georgia Institute of Technology, Atlanta, Georgia 30332, U.S.A.

(*Received* 1 *November* 1973)

Abstract—The layer structure of kaolinite from Twiggs, Georgia and fire-clay type kaolinite (Frantex B, from France), particle size separates 2–0·2 μm was studied by high resolution electron microscopy after embedment in Spurr low-viscosity Epoxy media and thin sectioning normal to the (001) planes by an ultramicrotome. Images of the (001) planes (viewed edge-on) of both kaolinites were spaced at 7 Å and generally aligned in parallel, with occasional bending into more widely spaced images of about 10 Å interval. Some of the 10 Å images converged to 7 Å at one or both ends, forming ellipse-shaped islands 80 to 130 Å thick and 300 to 500 Å long. The island areas and interleaved 10 Å layers between 7 Å layers may represent a residue of incomplete weathering of mica to kaolinite.

The proportions of micaceous occlusions were too small and the layer sequences too irregular to be detected by X-ray diffraction. The lateral continuity of the layers through the 7–10–7 Å sequence in a kaolinite particle would partially interrupt or prevent expansion in dimethyl sulfoxide (DMSO) and other kaolinite intercalating media. Discrete mica particles were also observed with parallel images at 10 Å, as impurities in both kaolinites. The small K content of the chemical analyses of the kaolinite samples is accounted for as interlayer K, not only in discrete mica particles but also in the micaceous occlusions.

INTRODUCTION

THIS study was planned to show the micromorphology and structural layers ("edge-on" view) of Georgia kaolinite and fire-clay type kaolinite and the presence of mica like wider spacings which may be related to non-expansion properties, by ultramicrotomy (UM) and high resolution electron microscopy (HREM). The so-called "fire-clay type kaolinite", described as having *b*-axis disorder, was found in a kaolinite from Tanganyika (Robertson *et al.*, 1954). An interleaved kaolinite, oriented with its cleavage parallel to that of the unaltered muscovite, was *b*-axis disordered (Jonas, 1964). A kaolinite which was not expanded by hydrazine (termed "intercalation disoder") was isolated from the fire-clay variety of kaolinite (Range *et al.*, 1969). Kaolinite minerals are frequently associated with considerable quantities of fine-grained quartz and mica, together with other impurities (Robertson *et al.*, 1954; Sayin *et al.*, 1971) which complicates interpretation of the chemical analysis, especially the K content of kaolinites.

The fringes of (001) crystal structures of chrysotile (Yada, 1967), muscovite (Brown and Rich, 1968), chlorite (Brown and Jackson, 1973), kaolinite (Lee *et al.*, 1972) and mixed layered kaolinite–montmorillonite (Lee *et al.*, 1973) were observed under HREM after thin sectioning with UM. The crystal structures of montmorillonite (Barclay and Thomson, 1969), organo–montmorillonite (Suito *et al.*, 1972), imogolite (Wada *et al.*, 1970), garnierites (Uyeda *et al.*, 1973) and interstratified mica-smectite (Yoshida, 1973) also were observed in portions of curved crystals with HREM.

MATERIALS AND METHODS

Relatively well-ordered kaolinite from Twiggs Co., central Georgia and the so-called "fire-clay" type of kaolinite (Frantex B, from France) were studied. The organic matter and amorphous material of samples was removed by P-free H_2O_2 and citrate–bicarbonate–dithionite (CBD) treatments (Jackson, 1969). The size fraction, 2–0·2 μm in diameter, was obtained from the sample by centrifugation and saturated with Mg^{2+} by 0·5 N $MgCl_2$ washings. After removal of excess salts by washings with 95% ethanol, the samples were dehydrated by washing with 100% ethanol and suspended in 100% ethanol approximately by the ratio of 1 ml cake volume:10 ml ethanol.

The embedment medium (an Epoxy, Spurr Low-Viscosity Embedding Media, Polysciences, Inc., Paul Valley Industrial Park, Warrington, PA 18976) was

* Post-Doctoral Associate and Franklin H. King Professor of Soil Science, respectively.

† Director.

prepared by gravimetric addition of the components into a plastic flask. The composition employed in this experiment was as follows: vinylcyclohexene dioxide, 10 g; diglycidyl ether of polypropyleneglycol, 5·0 g; nonenyl succinic anhydride, 26 g; and dimethylaminoethanol, 0·4 g. (Hardness of specimen block was controlled by adjustment of quantity of diglycidyl ether of polypropyleneglycol from 6 to 4 g, and 5 g was found to be optimal. With the smaller quantity, the hardness of block increased.) A layer of embedment medium, of thickness about 0·3 cm (about half of the well-mixed resin), was cast in a clean flat-bottom plastic vessel (about 9 cm dia.) and cured 8 hr in a 70°C oven.

The samples suspended in ethanol were mounted by a capillary tube in the flat-center area of the cured resin in the form of a thin (2 mm wide) strip and then dried at room temperature in a vacuum desiccator. The dried clay film was barely visible to the naked eye. A thin lead pencil line was drawn on an abraded area around each clay patch to make it easier to locate. A second layer of resin was then applied over a series of dried clay samples in a vacuum desiccator under vacuum (Fig. 1). The vacuum was released and the vessel left for an hour to allow the resin to permeate the samples. Then the vessel with resin and samples was transferred to an oven and cured in the same way as the first layer.

A specimen block was sawed from the resin "sandwich", filed to expose the edge of the clay patch, and glued with Epoxy cement to a standard cylindrical block for ultramicrotome cutting. After rough and precision trimming of specimen blocks, the truncated-pyramidal block face was decreased to be no longer than 0·6 mm on a side. The thin sections, less than 600 Å thickness were made perpendicular to (001) crystal planes by a Reichert ultramicrotome (OM-U2) and examined with a Phillips EM 200 electron microscope with a "microgun" source to minimize heating of the specimen and to improve contrast and resolution (Brown and Jackson, 1973). An accelerating voltage of 100 kV, through-focus technique, and magnification on the 35-mm film (Eastman P426) up to 83,000X were used. The magnification of the original electron micrograph was calibrated within an accuracy of ±1 per cent by a germanium-shadowed carbon replica of a diffraction grating (Brown and Jackson, 1973). Therefore, the spacings are recorded with an error on the order of ±0·1 Å. The selected areas of micrographs were enlarged about four times on glass slide plates, and then the spacings were recorded with an Automatic Recording Microdensitometer (Model MK III C, Joyce, Loebl and Co., Ltd.).

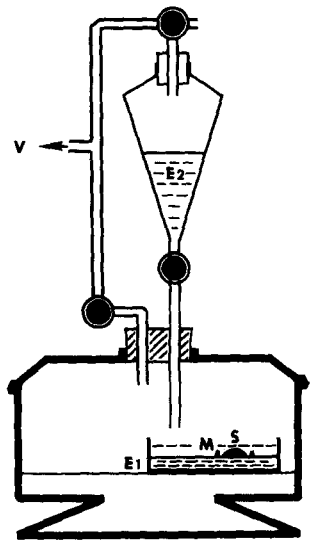

Fig. 1. Apparatus used for applying low-viscosity Epoxy (E_1, E_2) in vacuum (V). M = marking with lead pencil, S = sample (dried).

RESULTS

Micromorphology of kaolinites

The thin sectioned kaolinites from Georgia (GA) and France (FRA) ("fire-clay" or "Frantex B") were first examined at intermediate magnification (Fig. 2). The particle size of FRA kaolinite was relatively finer than that of GA kaolinite in the particle size range of 2–0·2 μm (Figs. 2a and b). An embedding method, based on centrifugation of the kaolinite suspension in the Epoxy liquid in a plastic bottle instead of previously drying the clay, yielded a gel with the kaolinite particles bent and widely spaced in the embedding media (Figs. 2c–e). Thin sections of the kaolinite were made from the bottom part of the Epoxy block after curing. The orientation of the kaolinite particles was random and the particles were extensively aggregated.

The GA kaolinite occurs as stacks or books, the thickness of individual crystallite packet being about 0·05–0·15 μm, or on the order of 100 crystal layers (Fig. 2f). Some of the packets do not extend to the edge of the particle, causing curvature of the neighboring packets (Fig. 2f). The embedding media penetrated into the spaces between kaolinite packets (Fig. 2f., arrow s). Such packets, referred to as "units of integral structures along the *Z* axis" and measured by an optical microscope were up to 0·15 μm thick, but most were near 0·04 μm (Conley, 1966). The kaolinite packets were not as thin as those of halloysite particles, measuring about 0·004–0·03 μm (Dixon and McKee, 1974).

Some of kaolinite particles were thin (high ratio length:thickness) and very flexible in the embedding media (Figs. 2d, e). When the flakes become thin enough, within a given particle size, the strength of interlayer bonds can no longer hold the layers rigid (Bates, 1971). The ratio of area or length to thickness of kaolinite particles is a useful parameter for morphological interpretation of the mode of kaolinite formation (Robertson *et al.*, 1954). The thin section technique therefore may be a reliable method for such studies as a supplement to the conventional shadow-casting technique.

https://doi.org/10.1346/CCMN.1975.0230208 Published online by Cambridge University Press

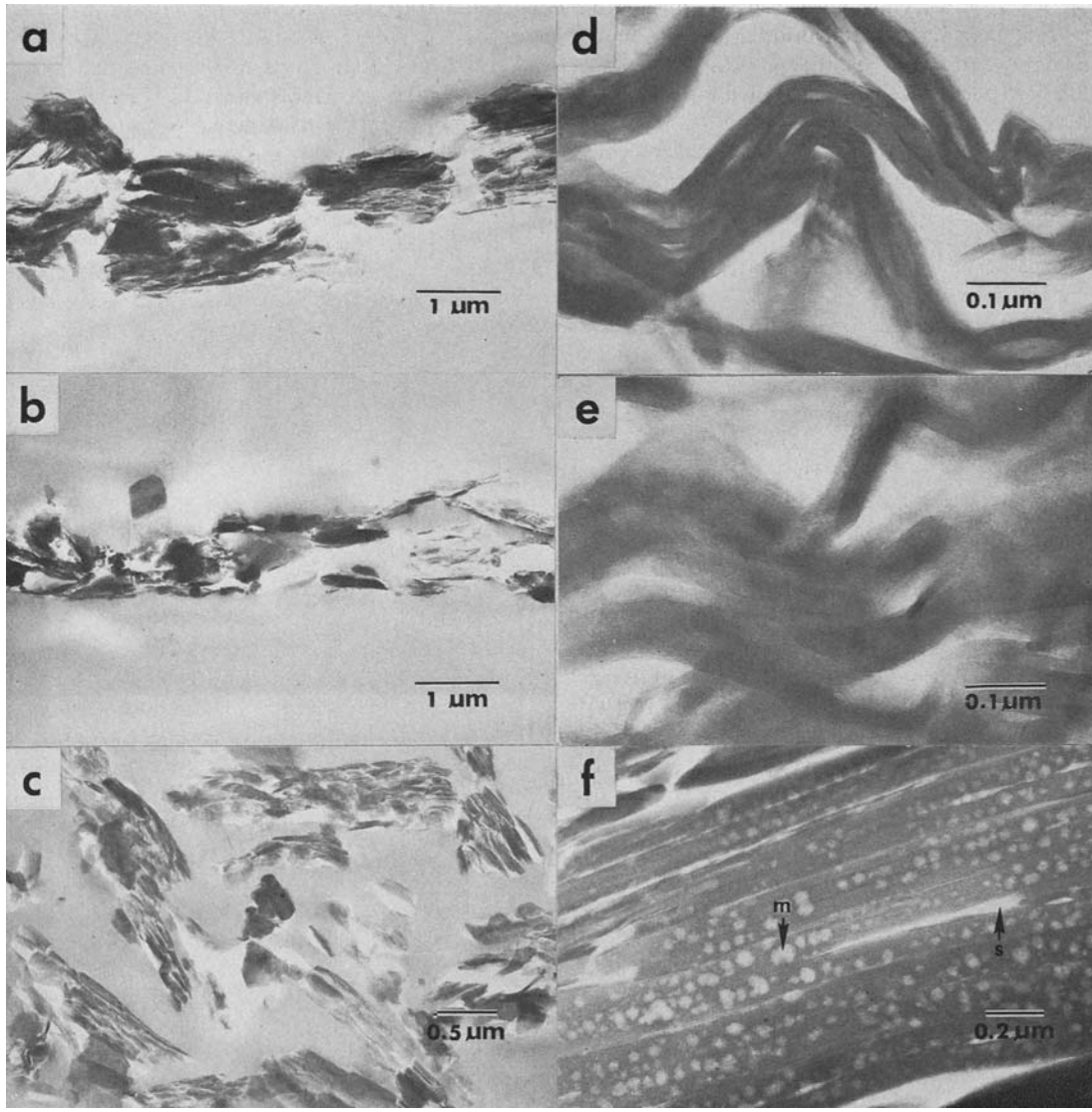

Fig. 2. Transmission electron micrographs of kaolinites from central Georgia (GA) and fire-clay (Frantex B) at intermediate magnification; (a) GA kaolinite embedded between two layers of embedding media, (b) Frantex B kaolinite embedded between two layers of embedding media, (c) GA kaolinite, showing gel-like nature in embedding media, (d) GA kaolinite, (e) Frantex B, showing flexibility of the thin kaolinite particles and (f) GA kaolinite, showing stacks and internal space (arrow s) in a particle, and electron beam damages (arrow m).

https://doi.org/10.1346/CCMN.1975.0230208 Published online by Cambridge University Press

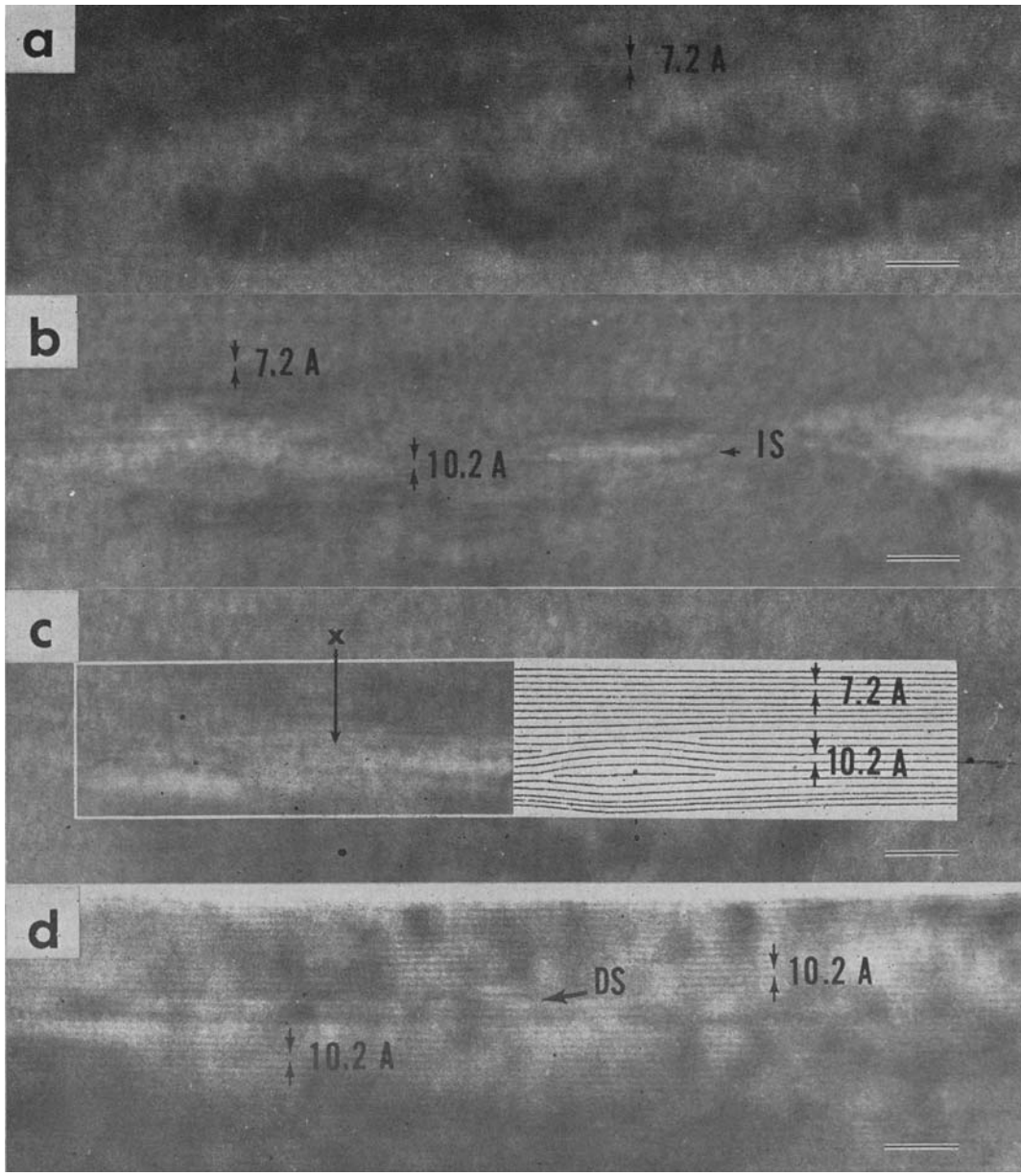

Fig. 3. High resolution electron micrographs of GA kaolinite thin sections; (a) typical kaolinite region spaced at 7·2 Å, (b) micaceous occlusions (IS) in kaolinite crystal matrix, (c) a micaceous occlusion and schematic presentation of the occlusion (arrow X representing approximate position of microdensitometer recording shown in Fig. 5) and (d) discrete mica particle in the kaolinite bulk sample, DS = dislocation. Scale marks = 100 Å.

https://doi.org/10.1346/CCMN.1975.0230208 Published online by Cambridge University Press

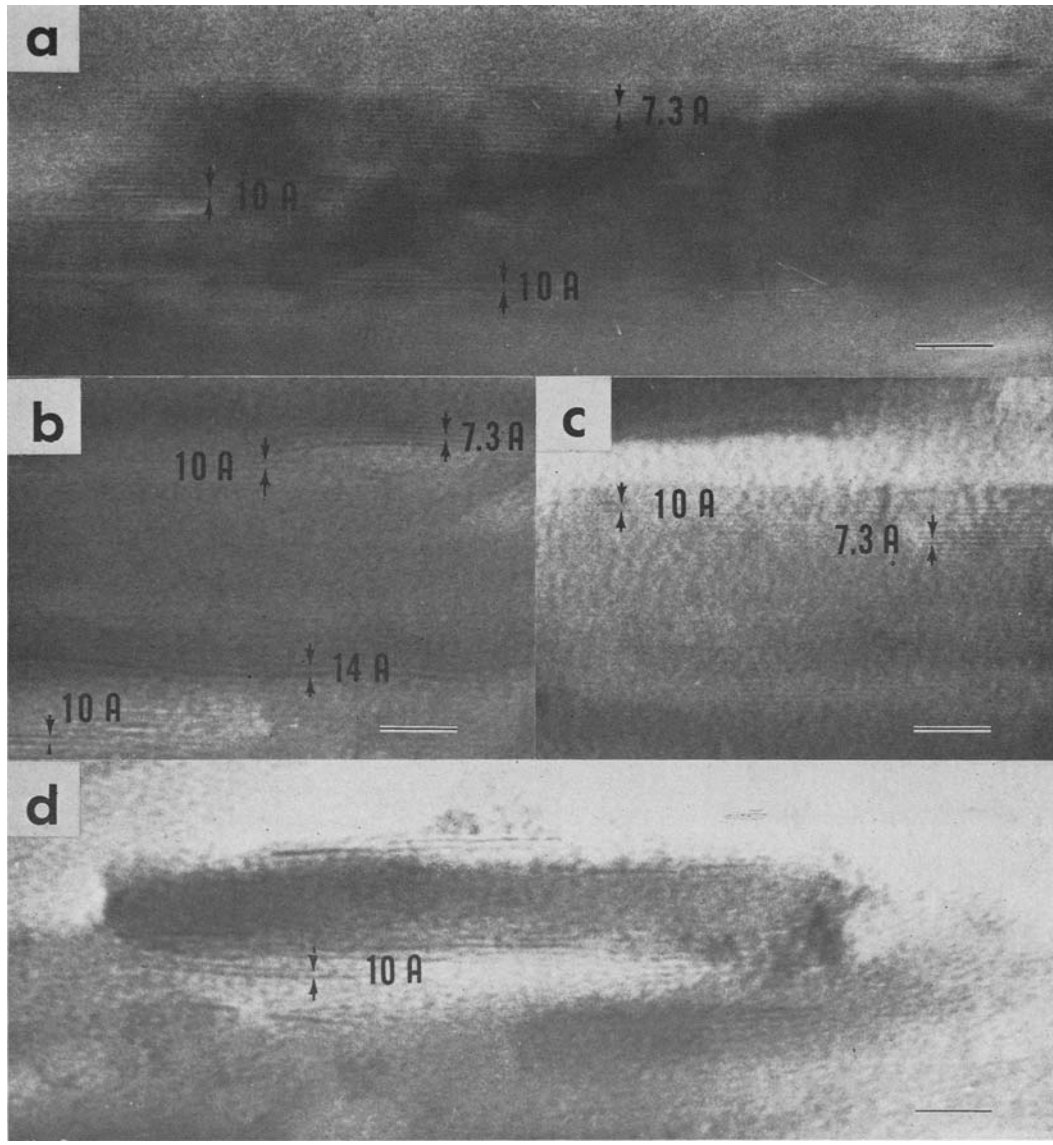

Fig. 4. High resolution electron micrographs of fire-clay kaolinite (Frantex B, France) thin sections; (a) typical kaolinite region spaced at 7·3 Å, with interleaved micaceous layers (10 Å), (b) and (c) micaceous layers in kaolinite crystal matrix and (d) partially weathered discrete mica particle in the kaolinite bulk sample. Scale marks = 100 Å.

https://doi.org/10.1346/CCMN.1975.0230208 Published online by Cambridge University Press

Because of a low thermal conductivity and the presence of structural hydroxyl in the kaolinites, heat produced by the electron bombardment during electron microscopic examination may initiate dehydration (mottling, Fig. 2f, arrow m). Such bombardment can cause the disappearance of (002) fringes of chlorite (Brown and Jackson, 1973), formation of voids and a rim on kaolinite (Chute and Amitage, 1968), and a loss of crystallinity in chrysotile (Yada, 1967). The damage by electron irradiation may be minimized, however, by use of a liquid N_2 cooling stage, lower beam current, a microgun source, and the through-focusing photographic technique to minimize the exposure time (Brown and Jackson, 1973).

Images of (001) *planes of kaolinites*

The fringes of numerous (001) crystal planes (viewed edge-on) of GA kaolinite are spaced at 7·2 Å and aligned in parallel (Fig. 3a). Some areas in a kaolinite image do not have fringes, which indicates that the thin section locally was too thick or was lying at an angle other than the Bragg angle to the electron beam. In thin sections of the FRA kaolinite, numerous fringes of (001) crystal spacings at 7·3 Å were observed (Fig. 4a). The image contrast of kaolinite fringes is relatively low, as compared to those of muscovite (Brown and Rich, 1968) and chlorite (Brown and Jackson, 1973). The image contrast depends on the kinds of atoms and the atomic positions in the mineral unit cell, as they affect the relative intensities of the direct and diffracted electron beams (Thomas, 1962) that are focused into the electron optical image. The intensity of the diffracted beam depends on the fulfillment of the Bragg equation and structural factor for diffraction (Brown and Jackson, 1973).

Micaceous occlusions in kaolinites

In the high resolution electron micrographs of thin sections of a GA kaolinite, ellipsoidal islands with more widely spaced fringes (about 10 Å) were often observed (Figs. 3b, c), occasionally formed by bending of the 7·2 Å (001) planes of kaolinite. Some of the 10 Å planes converged to 7·2 Å at one or both ends (Fig. 3b—also traced diagram). The size of the islands varied, ranging from 300 to 500 Å long and from 80 to 130 Å thick. The presence of the interleaved and occluded 10 Å spacings within 7 Å sequences was confirmed by microdensitometer measurements (Fig. 5). The micrograph was made by recording the density gradients normal to the fringes. For example, the Fig. 5 trace is marked by arrow X in Fig. 3c. Occasional fringes spaced at 10 Å, among 7 Å kaolinite spacings, were also revealed in thin sections of FRA kaolinite (Figs. 4a–c). The interleaved fringes spaced at 10 Å were oriented parallel to the numerous (001) kaolinite planes. Interleaved 14 Å fringes were occasionally observed in the thin sections of FRA kaolinites (Fig. 4b).

Discrete mica particles spaced at 10 Å were also observed as an impurity in both kaolinite samples

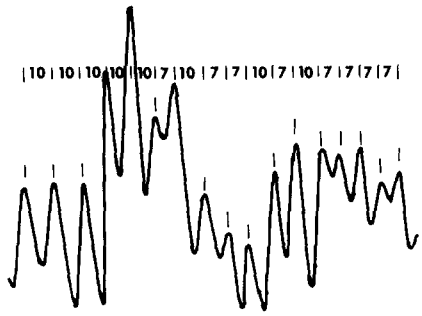

Fig. 5. Microdensitometer recording of a transect (arrow X in Fig. 3c), showing the presence of interleaved and occluded 10 Å fringes among 7 Å kaolinite fringes.

(Figs. 3d, 4d). After successive treatments with hexafluorotitanic acid, mica with other mineral impurities in GA kaolinite were isolated (Sayin *et al.*, 1971). The particle size of the mica isolated indicated occurrence as discrete mica particles as in Fig. 3d.

DISCUSSION

The observation of occluded and interleaved 10 Å structural fringes in 7 Å kaolinite matrix suggests the presence of micaceous layers in kaolinite particles. These micaceous layers may be a residual mica from which the kaolinite formed. In a related study, early stages of kaolinite formation from muscovite in bulk sedimentary GA kaolin was observed (Jonas, 1964) with a petrographic microscope as interleaved packets or along the outer edges and interior fractures of the altering sheaves of large muscovite grains.

The presence of 10 Å fringes, the K_2O content (2–0·2 μm fraction) of GA (0·075%) and FRA (0·065%) kaolinites, and the interference with the kaolinite intercalation (discussed below) support the interpretation that the 10 Å layers are micaceous mineral occlusions rather than hydrated halloysite. The (001) basal spacings of halloysites examined under similar conditions with HREM were 7·21–8·21 Å (McKee *et al.*, 1974). In similar Epoxy preparations (Lee *et al.*, 1973) interleaved micaceous layers (10 Å) were revealed in interstratified kaolinite–montmorillonite (21 Å), suggesting that the mixed mineral was a weathering product of micaceous mineral. The 14 Å spacing of FRA kaolinite (Fig. 4b) therefore can be interpreted as an interstratified vermiculite, montmorillonite, or chlorite.

A mechanism of kaolinite formation from montmorillonite under acid leaching of interlayer cations was proposed (Altschuler *et al.*, 1963) based on X-ray diffraction properties. Synchronous or immediately subsequent stripping off one silica sheet of montmorillonite, including the vacant tetrahedral oxygen sites, with replacement by hydroxyls was thought to create a highly polar kaolinite-like arrangement in the resulting 1:1 sheet. The layer charge from Al substitution for Si in the remaining tetrahedral sheet would be carried into the kaolinite with a few associated

interlayer cations between an octahedral and tetrahedral interlayer of the kaolinite. The kaolinite crystals may, alternately, have been nucleated as hydroxy aluminum units sorbed on the montmorillonite layers (Jackson, 1965).

The observation of the micaceous occlusions in kaolinites raises again the problem of characterizing fire-clay type kaolinite. The mineralogical term "fire-clay" was characterized as *b*-axis disordered kaolinite (Robertson *et al.*, 1954) and as "intercalation disordered kaolinite" (Range *et al.*, 1969). Range *et al.* (1969) successfully separated disordered (nonexpanding) kaolinite (Type IV) from expansible kaolinites in several kaolinites of different sources including GA and Frantex B (FRA) by a density separation technique. They claimed that the isolated kaolinite (Type IV) had isomorphous substitution of Al for Si in tetrahedra throughout the crystal, the charges of which were neutralized by interlayer cations such as K^+. The presence of the interlayer cations was presumed to prevent intercalation. Since the nonexpansible isolates would include unexpanded kaolinite particles which have occluded and/or interleaved micaceous minerals (Figs. 3c, 4a) as well as discrete mica particles (Figs. 3d, 4d), the nonexpanding kaolinite could represent a type with interlayer cations in mica remnants.

Interlayer cations could occur in interstratified kaolinite–mica layers as well as in the interlayer of micaceous mineral inclusions (Fig. 6) in kaolinite formed from micas. Vermiculite and montmorillonite both intercalate and swell in dimethyl sulfoxide (DMSO) and therefore interlayer cations associated with kaolinite layer charges (Fig. 6a) would not be expected to prevent the intercalation of kaolinite Type IV. The mica (or occasional chlorite) occlusions in the kaolinite, involving continuity of layers with a nonexpanding phase (mica, Figs. 6b, d) are more likely to prevent the penetration of an intercalation media through the interlayers of Type IV kaolinite.

CONCLUSIONS

1. Flexibility of kaolinite particles and their instability under the electron beam of the electron microscope were observed on the thin sections of kaolinites from GA and France (Fig. 2). The GA kaolinite occurs as "books" of 10–20 thin crystallites. An individual crystallite of kaolinite was about 0·1 μm thick, or on the order of a hundred 7 Å layers. Micropores caused by discontinuity within the books of kaolinite provide internal space in a particle for cation or anion adsorption sites and may influence exchange kinetic studies of kaolinites.

2. High resolution electron microscopy of ultramicrotomed sections of kaolinites revealed electron optical fringes of not only the expected 7 Å (001) spacing but also occasional 10 and 14 Å spacings. The 10 Å spacings were thought to represent occluded and interleaved mica. The 14 Å spacings may represent vermiculite, montmorillonite, or chlorite layers mixed in kaolinite crystals. The mica or chlorite occlusions are believed to prevent or interrupt expansion of these portions of the kaolinite particles in DMSO and other intercalating media.

3. In kaolinites derived from micaceous mineral, the interlayer K^+ can be allocated in several places; between kaolinite layers which have residual tetrahedral charges, in small occluded micaceous zones, between mica and kaolinite layers, and in discrete mica particles (Fig. 6). These micaceous residual high-charge zones may be significant in the retention of fixing cations.

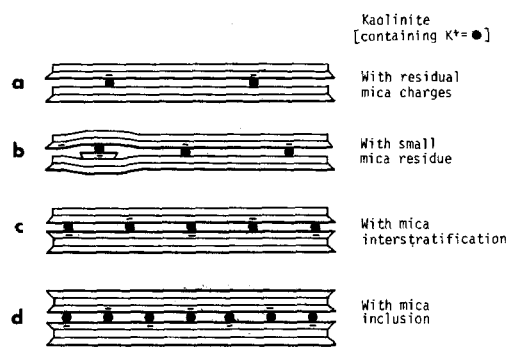

Fig. 6. Possible positions of interlayer cation (K^+) in a kaolinite particle which has been transformed from micas.

Acknowledgements—This research was supported by the School of Natural Resources, College of Agricultural and Life Sciences, University of Wisconsin, Madison; in part by the Ecological Sciences Branch, Division of Biomedical and Environmental Research, United States Atomic Energy Commission Contract AT(11-1)-1515-Jackson (paper COO-1515-44), under project 1336; in part by the J. M. Huber Corporation, Huber, GA and the National Science Foundation grant GA36219-Jackson, under project 1123; through an International Consortium for Interinstitutional Cooperation in the Advancement of Learning (ICICAL); in part by the Analytical Instrumentation Laboratories, Engineering Experiment Station, Georgia Institute of Technology. The authors are grateful to Professor A. Weiss, Institut für Anorganische Chemie der Universitat Munchen, for providing the Frantex B kaolinite, and to Mr. W. F. Abercrombie, J. H. Huber Corporation for providing the GA kaolinite samples.

REFERENCES

Altschuler, Z. S., Dwornik, E. J. and Kramer, H. (1963) Transformation of montmorillonite to kaolinite during weathering: *Science* **141,** 148–152.

Barclay, L. M. and Thompson, D. W. (1969) Electron microscopy of sodium montmorillonite: *Nature, Lond.* **222,** 263.

Bates, T. F. (1964) Geology and mineralogy of the sedimentary kaolins of the Southeastern United States: *Clays and Clay Minerals* **12,** 177–194.

Brown, J. L. and Jackson, M. L. (1973) Chlorite examination by ultramicrotomy and high resolution electron microscopy: *Clays and Clay Minerals* **21,** 1–7.

Brown, J. L. and Rich, C. I. (1968) High resolution electron microscopy of muscovite: *Science* **161,** 1135–1137.

Conley, R. F. (1966) Statistical distribution patterns of particle size and shape in the Georgia kaolins: *Clays and Clay Minerals* **14,** 317–330.

Chute, J. H. and Armitage, T. M. (1968) Alteration of clay minerals by electron irradiation: *Clay Minerals* **7,** 455–457.

Dixon, J. B. and McKee, T. R. (1974) Internal and external morphology of tubular and spheroidal halloysite particles: *Clays and Clay Minerals* **22,** 127–137.

Jackson, M. L. (1965) Clay transformation in soil genesis during the Quaternary: *Soil Sci.* **94,** 15–22.

Jackson, M. L. (1969) *Soil Chemical Analysis—Advanced Course.* 2nd Edition. Published by the author, Department of Soil Science, University of Wisconsin, Madison.

Jonas, E. C. (1964) Petrology of the Dry Branch, Georgia, kaolin deposits: *Clays and Clay Minerals* **12,** 199–207.

Lee, S. Y., Jackson, M. L. and Brown, J. L. (1972) Micaceous vermiculite domains in kaolinite observed by ultramicrotomy and high resolution electron microscopy: *Abstracts, 21st Clay Minerals Conf.* Woods Hole, Massachusetts.

Lee, S. Y., Jackson, M. L. and Brown, J. L. (1973) Micaceous vermiculite, glauconite, and mixed-layered kaolinite–montmorillonite examination by ultramicrotomy and high resolution electron microscopy: *Agronomy Abstracts,* American Society of Agronomy, Madison, Wisconsin, p. 150.

McKee, T. R., Dixon, J. B., Harling, D. F. and Whitehouse, U. G. (1974) Internal calibration of lattice resolution electron micrographs: *Abstracts, 23rd Clay Minerals Conf.* Cleveland.

Range, K. J., Range, A. and Weiss, A. (1969) Fire-clay kaolinite or fire-clay mineral? Experimental classification of kaolinite–halloysite minerals: *Proc 3rd Int. Clay Conf.* (Tokyo) **1,** 3–13.

Robertson, R. H. S., Brindley, G. W. and Mackenzie, R. C. (1954) Mineralogy of the kaolin clays from Pugu, Tanganyika: *Am. Miner.* **39,** 118–139.

Sayin, M., Jackson, M. L. and Syers, J. K. (1971) Anatase isolation from kaolinites by hydrofluotitanic acid and heavy liquids: *Abstracts, 20th Clay Minerals Conf.* Rapid City, South Dakota, p. 36.

Suito, E., Arakawa, M. and Yoshida, T. (1969) Electron microscopic observation of the layer of organo-montmorillonite: *Proc. 3rd Int. Clay Conf.* (Tokyo) **1,** 757–763.

Thomas, G. (1962) *Transmission Electron Microscopy of Metals.* Wiley, New York.

Uyeda, N., Hang, P. T. and Brindley, G. W. (1973) The nature of garnierites–II. Electron-optical study: *Clays and Clay Minerals* **21,** 41–50.

Wada, K., Yoshinaga, N., Yotsumoto, H., Ibe, K. and Aida, S. (1970) High resolution electron micrographs of imogolite: *Clay Minerals* **8,** 487–489.

Yada, K. (1967) Study of chrysotile asbestos by a high resolution electron microscope: *Acta Cryst.* **23,** 704–707.

Yoshida, T. (1973) Elementary layers in the interstratified clay minerals as revealed by electron microscopy: *Clays and Clay Minerals* **21,** 413–420.